Conformational Equilibria of Terminally Blocked Single Amino Acids at the Water−Hexane Interface. A Molecular Dynamics Study

Christophe Chipot[†,‡] and Andrew Pohorille*[,†,§]

Exobiology Branch, NASA−Ames Research Center, MS 239-4, Moffett Field, California 94035-1000, and Department of Pharmaceutical Chemistry, University of California, San Francisco, San Francisco, California 94143-0446

Received: March 13, 1997; In Final Form: July 28, 1997[⊗]

The conformational equilibria of the acetyl and methyl amide terminally blocked L-alanine, L-leucine and L-glutamine amino acids are examined in vacuum, in bulk water, and at the water−hexane interface, using multi-nanosecond molecular dynamics simulations. The two-dimensional probability distribution functions of finding the peptides at different dihedral angles of the backbone, ϕ and ψ, are calculated, and free energy differences between different conformational states are determined. All three peptides are interfacially active, i.e. tend to accumulate at the interface even though they are not amphiphilic. Conformational states stable in both gas phase and water are also stable in the interfacial environment. Their populations, however, cannot be simply predicted from the knowledge of conformational equilibria in the bulk phases, indicating that the interface exerts a unique effect on the peptides. Conformational preferences in the interfacial environment arise from the interplay between electrostatic and hydrophobic effects. As in an aqueous solution, electrostatic solute−solvent interactions lead to the stabilization of more polar peptide conformations. The hydrophobic effect is manifested at the interface by a tendency to segregate polar and nonpolar moieties of the solute into the aqueous and the hexane phases, respectively. For the terminally blocked glutamine, this favors conformations for which such a segregation is compatible with the formation of strong, backbone−side chain intramolecular hydrogen bonds on the hexane side of the interface. The influence of the hydrophobic effect can be also noted in the orientational preferences of the peptides at the interface. The terminally blocked leucine is oriented such that its nonpolar side chain is buried in hexane, whereas the polar side chain of glutamine is immersed in water. The free energies of rotating the peptides along the axis parallel to the interface by more than 90° are substantial. This indicates that peptide folding at interfaces is strongly driven by the tendency to adopt amphiphilic structures.

1. Introduction

Amino acids terminally blocked by acetyl (Ac−) and methyl amide (−NHMe) groups contain one side chain but two peptide bonds. They are, therefore, often referred to as "dipeptides".[1] Studies of these model systems provide direct information about the intrinsic conformational preferences of an isolated peptide unit, separating them from effects involving side chain−side chain and long-range backbone interactions. The idea that a thorough knowledge of the conformational behavior of a single peptide unit may contribute significantly to the overall understanding of peptide folding motivated numerous studies of the terminally blocked alanine in the gas phase and in an aqueous solution using a variety of theoretical techniques, such as self-consistent reaction field ab initio calculations,[2−4] computer simulations,[1,5−13] and integral equation theory.[14,15] These studies yielded new, significant results about the influence of solvent and intramolecular hydrogen bonding on the conformations of peptides.

In the present work, the previous investigations are extended by considering blocked amino acids in an interfacial aqueous environment. Our main objectives are to determine whether these molecules tend to accumulate at the interface and how the intrinsic conformational and orientational preferences of an isolated peptide unit are influenced by the anisotropic interfacial environment and the side chain polarity.

The motivation for this study is provided by the biological and pharmaceutical importance of membrane-bound peptides[16−23] and small protein fragments[24−26] which show affinity to the water−membrane interface. This anisotropic, complex environment exerts a strong organizing effect on peptide structures by driving many peptides, which are typically disordered in an aqueous solution in their monomeric form, to sequence-dependent, preferred conformations at the interface. One possible approach to understanding this effect is to consider short, synthetic peptides, designed to probe different aspects of peptide−membrane interactions.[27−32] In particular, the interactions of a series of tripeptides with dimyristoylphosphatidylcholine (DMPC) bilayers were studied to elucidate the role of individual amino acids in peptide−lipid interactions.[29,31,33] Studies on longer, synthetic peptides demonstrated that, depending on their sequence, they are capable of adopting all major structural motifs found in proteins, including α-helices,[28,30,34−36] β-strands,[37] and β-turns.[38]

In spite of this considerable, recent progress, the relationship between the sequence of the peptide and its conformation at

† NASA−Ames Research Center.
‡ On leave from: Laboratoire de Chimie Théorique, Unité de Recherche Associée au CNRS No. 510, Université Henri Poincaré-Nancy I, BP. 239, 54506 Vandœuvre-lès-Nancy Cedex, France.
§ University of California, San Francisco.
⊗ Abstract published in *Advance ACS Abstracts,* December 1, 1997.

S1089-5647(97)00938-3 CCC: $15.00
Published on Web 01/01/1998

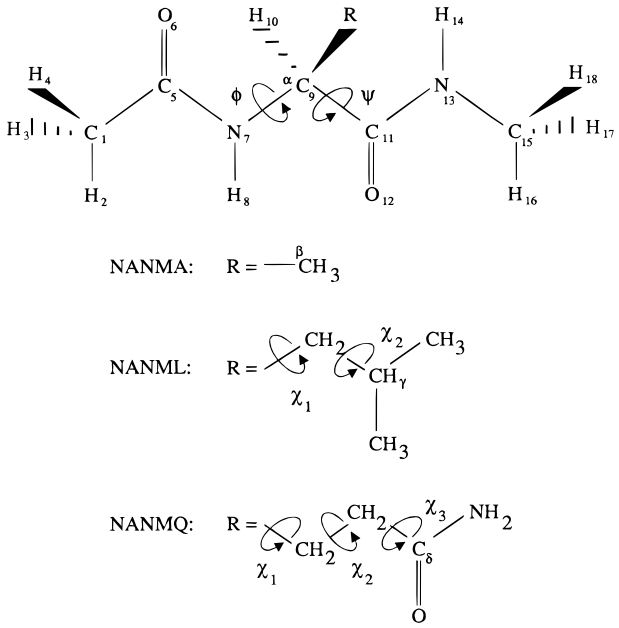

Figure 1. Ac− and −NHMe terminally blocked single amino acids *N*-acetyl-N′-methyl-L-alanylamide (NANMA), *N*-acetyl-*N*′-methyl-L-leucylamide (NANML), and *N*-acetyl-*N*′-methyl-L-glutamylamide (NANMQ).

the interface is not well understood. Studying the intrinsic conformational and orientational preferences of blocked amino acids can be considered as the first step on a path toward gaining a better understanding of this relationship. Subsequently, the results on longer peptides can be analyzed in terms of a sum of these intrinsic preferences and long-range effects involving both the backbone and the side chains.

In this paper, we present results on the conformational equilibria of three terminally blocked single amino acids: the *N*-acetyl-*N*′-methyl-L-alanylamide (NANMA) and its L-leucyl (NANML) and L-glutamyl (NANMQ) analogues. They were investigated using multi-nanosecond molecular dynamics computer simulations. The molecules are drawn schematically in Figure 1. This choice of molecules allows us to study the influence of polar and nonpolar side chains on the conformational and orientational preferences of a single peptide unit and is motivated by our interest in the interfacial behavior of nonpolar and amphiphilic peptides. The present work is a continuation of our previous studies of NANMA at the water−hexane[11] and the water−membrane[39] interfaces and has recently been extended to blocked dipeptides built of L-leucine, L-glutamine, and L-alanine, the undecamer of poly-L-leucine, and oligopeptides with different sequences of L-leucine and L-glutamine.[40]

As a model interfacial environment, we selected the water−hexane, rather than the water−membrane, system. This choice allows us to study the role played by the interface between polar and nonpolar phases without the complications arising from the slow relaxation of collective motions of lipid molecules accompanying conformational changes in the peptides.[39] Clearly, several effects that may influence the behavior of peptides at the water−membrane interface are absent in the water−hexane system. Among them are electrostatic interactions between phospholipid head groups and charged amino-acid side chains, which hold the peptides at the bilayer surface.[41,42] Also absent are the reorganization effects in the bilayer resulting from the incorporation of the solute into the head group region of the membrane,[43] and closely related effects of the curvature of vesicles on the partitioning of peptides into bilayers.[44] Despite these differences, however, many solutes, including peptides, exhibit qualitatively similar behavior at different interfaces between water and nonpolar media. These similarities are largely due to the importance of the balance between hydrophilic interactions with the aqueous environment and hydrophobic interactions with the nonpolar phase, as pointed out for peptides[45] and analyzed in detail for small solutes.[46] This is underscored by findings that peptides built of different sequences of leucine and lysine form the same secondary structures at the water−membrane, water−air, and water−hydrocarbon interfaces.[27,36,47] In another example, it was found in computer simulations that the distributions of anesthetic compounds across the water−hexane and water−glycerol 1-monooleate (GMO) bilayer are very similar, but differ from the distributions of nonanesthetics.[48−50] The identical conclusion was subsequently reached from NMR studies of anesthetics and nonanesthetics at the water−phospholipid bilayer interface.[51,52] Perhaps most relevant to the present work are similarities in the conformational equilibria of NANMA at the water−hexane[11] and water−GMO bilayer,[39] which will be further discussed in this paper.

Studies of solute partitioning into the water−hexane interface should be clearly distinguished from approaches in which binding of solutes to the membrane is modeled as partitioning from water into the bulk, organic phase. Since partitioning into interfacial environments is quite different than into bulk liquids, these two approaches yield qualitatively different results. The difference can be readily appreciated by noting that the solubilities of a broad range of anesthetic compounds at the water−hexane and water−membrane interfaces, but not in bulk hexane, octanol, and olive oil, correlated well with their anesthetic potencies.[50] This illustrates a repeatedly emphasized point: bulk-phase measurements are inadequte for describing interactions of solute molecules with membrane bilayers.[43,32]

2. Method

2.1. Description of the Systems. The interfacial systems were placed in a simulation box, the dimensions of which were 24 × 24 Å in the *x*,*y*-plane, parallel to the interface, and 200 Å along the *z*-direction, perpendicular to the interface. Periodic boundary conditions were applied in all three directions. The systems consisted of a lamella of 518 water molecules between two hexane lamellae, each containing 54 molecules. The width of each of the three lamellae was approximately 24 Å. The hexane lamellae were in equilibrium with their vapor phases. In this arrangement, the system contained two water−hexane interfaces. One blocked amino acid was placed at each interface. Thus, two, well-separated, solute molecules were simultaneously studied in a single molecular dynamics simulation. To ensure that the peptides did not partition to the bulk phases, soft restraining potentials along *z* kept the solutes within ±5 Å from the interface.

The bulk aqueous solution of the peptides was simulated as a cubic box containing 476 solvent molecules and one solute molecule. The edge length of the box was 24.4 Å. Periodic boundary conditions were applied in the three spatial directions.

2.2. Potential Energy Functions. Water molecules were described by the TIP4P model.[53] To represent hexane molecules the OPLS model[54] was used. In this approach, the aliphatic CH_n groups were treated as electrically neutral united atoms, the total mass of which was centered on the carbon atoms. The water−hexane Lennard-Jones parameters were derived from the standard OPLS combination rules.[54] The bond lengths and valence angles of the water and hexane molecules were constrained to their equilibrium values, using the SHAKE algorithm.[55]

Each blocked peptide was represented by a flexible, all-atom model. Both the inter- and intramolecular parameters for the three solutes were taken from the AMBER force field of Cornell et al.[56] This force field contains contributions from deformation of chemical bond lengths and valence angles, rotation of dihedral angles, and Coulomb and Lennard-Jones interactions between nonbonded atoms. The Lorentz−Berthelot combination rules were used to obtain Lennard-Jones parameters for the peptide−water and the peptide−hexane potential energy functions. The point charges on atoms of each blocked amino acid were distributed into small, electrically neutral groups.[57] Intermolecular interactions between groups and/or water molecules were smoothly truncated between 7.5 and 8.0 Å, using a cubic spline function.

2.3. Molecular Dynamics Free Energy Calculations. All the molecular dynamics simulations were carried out in the microcanonical ensemble, using the COSMOS program.[58] The equations of motion were integrated using the Verlet algorithm[59,60] with a time step of 2 fs for the interfacial systems, 2.5 fs for the bulk solutions, and 1 fs for peptides in the gas phase. The temperature was maintained at 300 K by occasionally rescaling the velocities.

Each set of simulations was designed to calculate the two-dimensional probability distribution function, $P(\phi,\psi)$, for finding a peptide in a conformation described by the flexible backbone dihedral angles ϕ and ψ (see Figure 1). For the peptides located in the gas phase, or at the water−hexane interface, $P(\phi,\psi)$ was obtained for the full range of angles ϕ and ψ. In the simulations of the three solutes in bulk water, the values of the backbone dihedral angles were limited to $-215° \le \phi \le +5°$ and $-85° \le \psi \le +215°$. This range includes the α_R, β, C_{7-eq}, and C_5 states, but not α_L and C_{7-ax}. As has been previously pointed out in the case of NANMA,[10] only the α_R and β states are significantly populated in the aqueous solution. Thus, the imposed restrictions do not limit our ability to determine the populations of the most stable conformers in water.

To obtain $P(\phi,\psi)$ the "umbrella sampling" technique[61] was used. The range of values accessible to ϕ and ψ was divided into a series of overlapping "windows".[62] Separate molecular dynamics trajectories were obtained, in which the solute was constrained to the backbone conformations within each window by applying a restraining harmonic potential outside the window. In some cases a biasing potential was added to the potential energy to ensure a more uniform sampling of the backbone dihedral angles within the window, thereby improving the statistical accuracy of the resulting probability distribution. Approximately 8−12 windows were required to cover the full range of ϕ and ψ. On average, two consecutive windows overlapped by 30° in ϕ or ψ. For each peptide at the water−hexane interface, approximately 14 ns of molecular dynamics trajectories were generated. The total simulation length was approximately 12 ns for a peptide in vacuum and 9 ns for a peptide in water.

In each window, a two-dimensional histogram of the backbone angles was accumulated. The complete probability distributions were built by matching the unbiased histograms in their overlapping regions, using the two-dimensional weighted histogram analysis method (WHAM).[63] These distributions were subsequently integrated over the ranges of ϕ and ψ characteristic of the α_R, β, C_{7-eq}, C_5, C_{7-ax}, and α_L conformational states. This yielded the unbiased free energy differences, $\Delta A_{a\to b}$, between states "a" and "b":

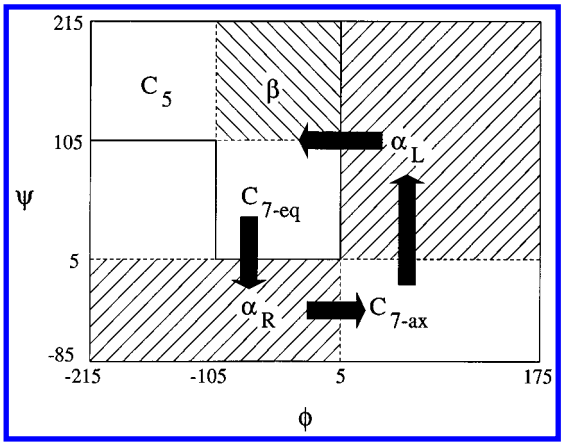

Figure 2. Topological definition of the pathway used in the free energy calculations.

$$\Delta A_{a\to b} = -k_B T \ln \frac{\int_{\phi_b}\int_{\psi_b} P(\phi,\psi)\, d\phi\, d\psi}{\int_{\phi_a}\int_{\psi_a} P(\phi,\psi)\, d\phi\, d\psi} \qquad (1)$$

where k_B is the Boltzmann constant and T is the temperature of the system.

The definitions of the conformational states are illustrated in Figure 2. The values of ϕ and ψ, considered typical to each state, always lie within the defined range. The choice of angles separating different conformational states is, however, somewhat arbitrary. In most instances, these angles correspond to the low probability regions in $P(\phi,\psi)$, and therefore, their exact values have only negligible effects on the calculated free energy differences. The only ambiguity exists in the region of β, C_{7-eq}, and C_5, since these states are not always separated by well-defined free energy barriers. We, thus, defined a β' conformational state that covers the ϕ and ψ ranges of these three states. In some instances, it is more convenient to discuss the conformational equilibria in terms of this broadly defined state rather than the three participating conformations.

To calculate statistical errors, molecular dynamics trajectories for each window were divided into blocks, and separate $P(\phi,\psi)$ were constructed from histograms in each block. This was done by using the two-dimensional WHAM. For each of these probability distributions the free energy differences were calculated using eq 1. Statistical errors were obtained by treating these free energy differences as uncorrelated measurements. Using this method, the error in calculating the free energy difference between the α_R and β' states of NANML in the gas phase and in water is 0.1 kcal/mol. At the interface, the statistical error is somewhat larger, 0.3 kcal/mol. Similar errors were obtained for NANMA and NANMQ.

3. Results and Discussion

3.1. Conformational Equilibria in the Gas Phase. The free energies of different conformational states of the three peptides, obtained from the integration of $P(\phi,\psi)$ over the regions of ϕ, ψ depicted in Figure 2, are listed in Table 1. From the probability distributions shown in Figure 3, we see that the only stable states are C_{7-eq}, C_5, and C_{7-ax}. C_{7-eq} and C_5, however, are separated only by a low free energy barrier, smaller than 1 kcal/mol. In all stable conformations, the backbone atoms form an intramolecular hydrogen bond. In C_{7-eq} and C_{7-ax} the $O_6\cdots H-N_{13}$ bond is a part of a seven-membered ring, whereas in C_5 the $N_7-H\cdots O_{12}$ hydrogen bond is in a five-membered ring.

TABLE 1: Relative Free Energy Differences between Key Conformations of NANMA, NANML, and NANMQ in Vacuo, Derived from the Two-Dimensional WHAM[63] Probability Distributions

	ΔA (kcal/mol)		
	NANMA	NANML	NANMQ
α_R	0.0	0.0	0.0
β	−1.3	−2.2	0.6
C_5	−1.5	−2.2	0.0
C_{7-eq}	−2.1	−2.9	−1.3
C_{7-ax}	−0.3	−1.2	−0.7
α_L	3.9	4.3	2.4
β'^a	−2.4	−3.1	−1.4

[a] β' denotes the portion of the (ϕ, ψ) map encompassing the β, C_5, and C_{7-eq} states.

TABLE 2: Relative Free Energy Differences between the β and the α_R Conformations of NANMA, NANML, and NANMQ in Bulk Water, Derived from the Two-Dimensional WHAM[63] Probability Distributions

	ΔA (kcal/mol)		
	NANMA	NANML	NANMQ
α_R	0.0	0.0	0.0
β	0.0	0.3	−0.3
C_5	0.8	1.3	0.5
C_{7-eq}	1.6	1.7	1.2
β'^a	−0.1	0.2	−0.8

[a] β' denotes the portion of the (ϕ, ψ) map encompassing the β, C_5, and C_{7-eq} states.

Among the stable conformations, C_{7-eq} always possesses the lowest free energy. In NANMA and NANML this conformational state is favored over C_{7-ax} by 1.8−1.9 kcal/mol. This agrees well with previous molecular dynamics simulations of NANMA,[10,11] which yielded the free energy difference between the two conformations in the range 1.5−2.0 kcal/mol. The relative free energies of the stable conformations in Table 1 are also close to those obtained by Gould et al.[4] from MP2/TZVP quantum mechanical calculations including HF/6-31G**//HF-6-31G** zero-point energy, thermal, and entropic corrections. Note, however, that the comparisons are made between slightly different quantities since stable conformations were defined in the previous statistical and quantum calculations as corresponding to the free energy minima rather than different regions of the ϕ, ψ conformational space.

Similarities in conformational preferences of NANMA and NANML are not limited to the relative free energies of the stable states but extend to $P(\phi,\psi)$ over the full range of ϕ and ψ. For NANMQ, the probability distribution is slightly different. Relative to C_{7-eq}, C_{7-ax} is more stable and C_5 is less stable than in NANMA and NANML. These differences are due to additional intramolecular hydrogen bonds that can form between the backbone and the side chain of NANMQ but not NANML and NANMA. In particular, a strong hydrogen bond between N_7−H and O═C_δ stabilizes C_{7-ax}. The corresponding values of the side chain torsional angles χ_1 and χ_2 are centered about −60°. In C_{7-eq}, the N_7−H···O═C_δ hydrogen bond still dominates but is less frequent and is associated with a different set of χ angles.

3.2. Conformational Equilibria in Bulk Water. When comparing $P(\phi,\psi)$ for the three blocked amino acids in a vacuum and in water, as shown in Figure 3, it can be observed that the C_{7-eq} and C_5 states are destabilized in the aqueous solution. At the same time, the more open conformations, α_R and β, gain stability. The depopulation of the C_{7-eq} and C_5 states results from the disruption of the intramolecular hydrogen bonds in the peptides by the surrounding water molecules, which effectively compete for access to the polar groups in the backbone, all of which are capable of hydrogen bonding. This observation agrees with the results of circular dichroism measurements of NANMA in water.[64] From these measurements, it was concluded that the population of the C_{7-eq} region, which predominates in chloroform, is redistributed in water between the β and the α_R conformations.

The relative free energies of different conformational states are given in Table 2. For all three blocked amino acids, the two stable conformations, α_R and β, are almost equally populated. For the nonpolar NANML, α_R is slightly more stable, whereas β is favored for the polar NANMQ. NANMA represents an intermediate case, where the free energy difference between α_R and β is zero. This agrees well with the estimate of 0.2 kcal/mol made for this difference by Tobias and Brooks.[10]

The almost identical free energies of α_R and β for all three peptides in water, but not in the gas phase, indicate that the solvent affects differently the conformational equilibria in each peptide. In discussing how the solvent effect changes in different environments, the β' state is considered rather than β, because the former includes conformations stable in both the gas phase and water. The free energy of solvation of β', relative to α_R, calculated as the difference between the free energies of this state in water and in vacuum, given in Tables 1 and 2, is positive for all three peptides. Compared to α_R, β' is destabilized by the solvent by 3.1 kcal/mol for NANML, but only by 0.6 kcal/mol for NANMQ. NANMA again falls between those two; the difference in the solvent effect for this peptide is equal to 2.2 kcal/mol. Several factors contribute to the observed differences in the free energy of solvation. The most important among them is probably the change in the solute−solvent electrostatic free energy caused by a change in the solute polarity. In NANML, the transition from α_R to β' is associated with a substantial reduction of the average molecular dipole moment from ca. 8 D to 4.3 D. This, in turn, leads to a considerable decrease of the favorable electrostatic contribution to the solvent effect. In NANMQ, not only the backbone but also the polar side chain contributes importantly to the molecular dipole moment, which is reduced by only 1.3 D. The resulting influence on the solvent effect is, thus, likely to be small. This qualitative explanation of the differences in the solvent effect follows an argument by Tobias and Brooks,[10] who noted that the transition between β and α_R is accompanied by a reorientation of the local peptide bond dipole moments from antiparallel to parallel.

For all three blocked amino acids, α_R is separated from β by a considerable free energy barrier. This barrier is equal to 2.8 kcal/mol for NANMA and NANMQ and is somewhat higher for NANML (3.6 kcal/mol). For the latter, the distributions of χ_1, χ_2, and χ_2' remain unaffected during the transition between the β and α_R. For NANMA, the barrier is located at $\psi \simeq 50°$, and at $\psi \simeq 30°$ for the remaining two peptides.

3.3. Conformational and Orientational Equilibria at the Water−Hexane Interface. In Figure 4, we show how the free energy of the three blocked amino acids in the α_R and β conformations changes along the *z*-direction, perpendicular to the interface. Since we imposed restraints on the solutes to keep them in the interfacial environment, the free energy has been determined only within these restraints, and the free energies of transfer from the bulk phases to the interface have not been established. It is, nevertheless, clear from the free energy profiles that all three amino acids exhibit free energy minima near the interface and, therefore, should be considered

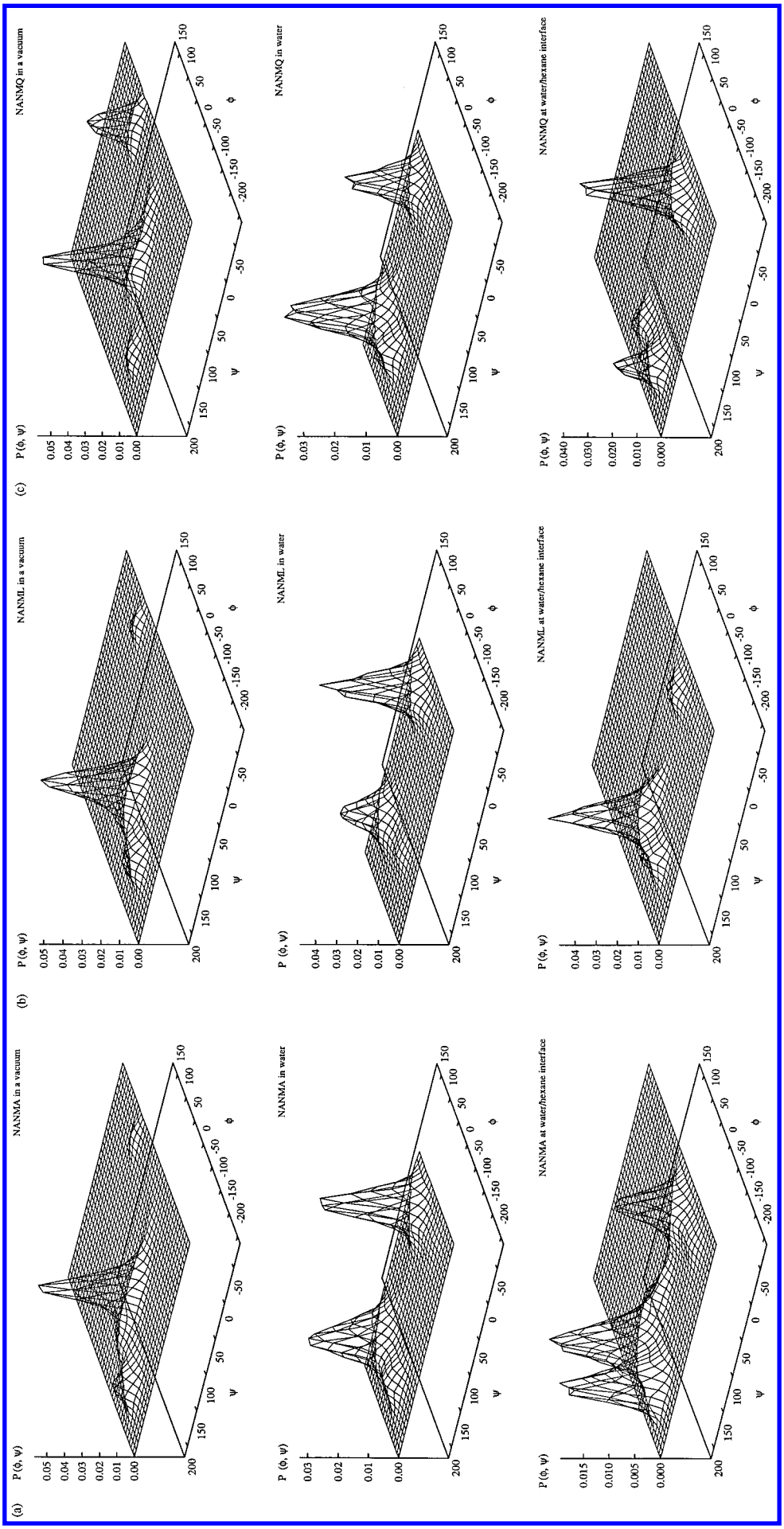

Figure 3. Two-dimensional probability distributions of finding NANMA (a), NANML (b), and NANMQ (c) at different values of the backbone dihedral angles ϕ and ψ, in the gas phase (top), in an aqueous solution (middle), and at the water−hexane interface (bottom).

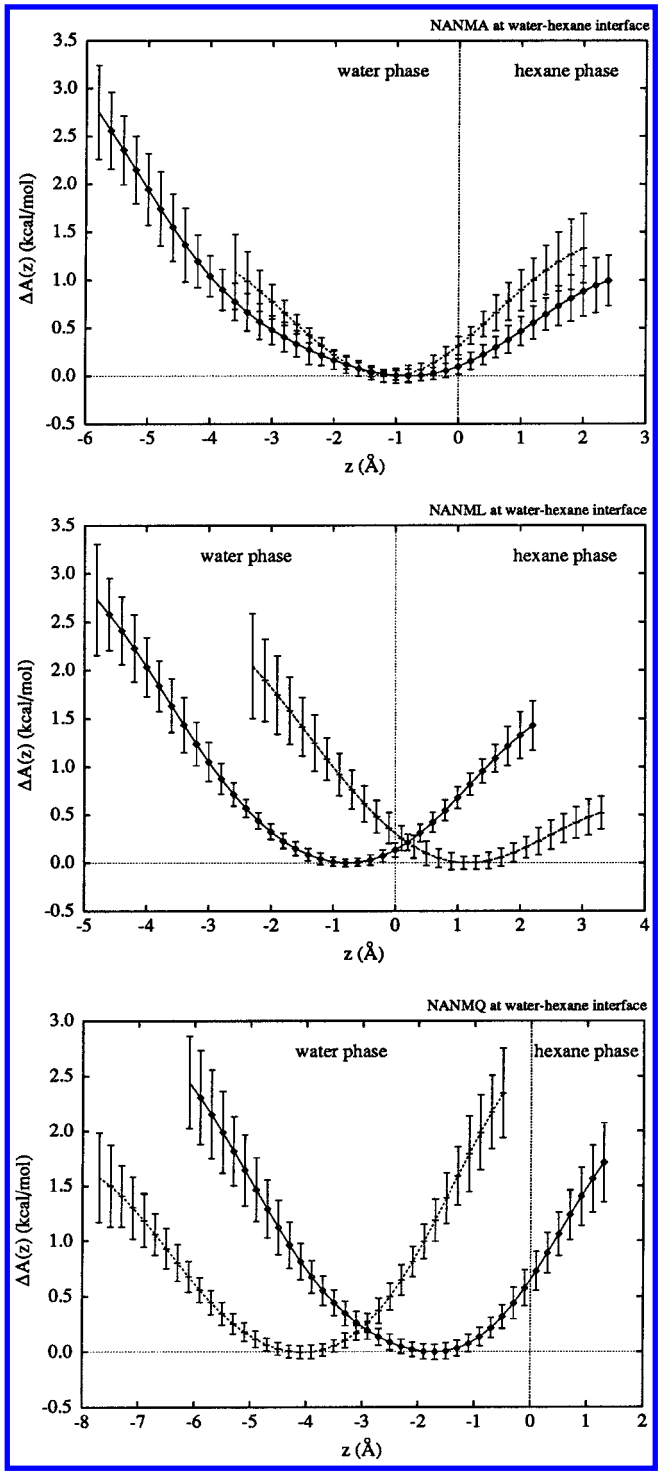

Figure 4. Free energy of the α-carbon of NANMA (top), NANML (middle), and NANMQ (bottom), as a function of z, the direction perpendicular to the interface. Only the α_R (solid line) and the β (dashed line) states are displayed.

interfacially active. A similar behavior was observed in the computer simulations of NANMA at the water−membrane interface.[11] This is due to the presence of both polar and nonpolar groups in the solute. As discussed recently,[46] this appears to be a sufficient condition for interfacial activity of small, although not necessarily amphiphilic, solutes. As the solute is moved from water to hexane, the free energy of creating a cavity that accommodates the solute decreases, whereas the solute−solvent electrostatic free energy increases. The sum of these two contributions exhibits a minimum at the interface, which, at a high dilution, is equivalent to an increased interfacial concentration. In NANML, the balance between the nonpolar side chain and the polar carbonyl and amino groups in the backbone stabilizes the peptide at the interface. For NANMQ, which has a polar side chain, interfacial activity is ensured by the presence of the hydrophobic terminal blocking groups.

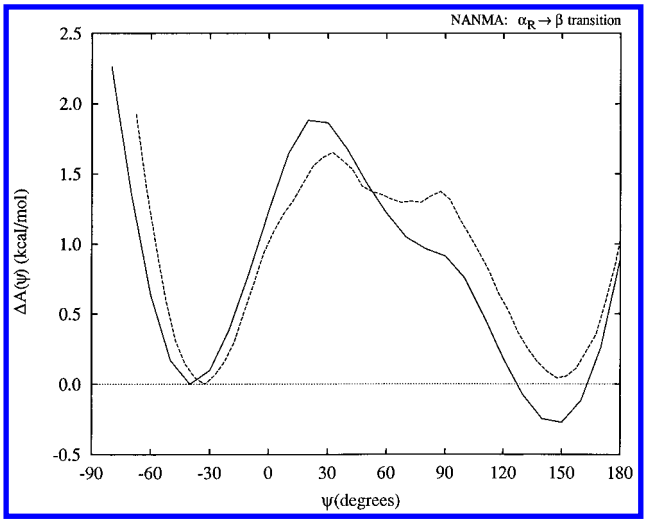

Figure 5. Free energy for the $\alpha_R \leftrightarrow \beta$ isomerization of NANMA at the water−hexane (solid line) and water−GMO (dashed line) interfaces.

TABLE 3: Relative Free Energy Differences between Key Conformations of NANMA, NANML, and NANMQ at the Water−Hexane Interface, Derived from the Two-Dimensional WHAM[63] Probability Distributions

	ΔA (kcal/mol)		
	NANMA	NANML	NANMQ
α_R	0.0	0.0	0.0
β	−0.3	−1.1	1.1
C_5	−0.3	−0.4	0.6
C_{7-eq}	0.7	−0.1	2.3
C_{7-ax}	2.8	2.0	2.8
α_L	4.1	3.7	4.1
β'^a	−0.7	−1.3	0.3

[a] β' denotes the portion of the (ϕ, ψ) map encompassing the β, C_5, and C_{7-eq} states.

To assess the influence of the specific chemical nature of the interfacial environment on conformational equilibria of blocked amino acids, we compare the free energy profiles for the $\alpha_R \leftrightarrow \beta$ isomerization of NANMA at the water−hexane and water−GMO bilayer interfaces. As can be seen from Figure 5, these two profiles are quite similar. Although the GMO head group is chemically simpler than the head group of a phospholipid and its atoms typically carry smaller partial charges, the surface potential of the GMO bilayer is of the same order of magnitude than that of many phospholipids (ca. 0.3 V).[65] Thus, electrostatic effects of both interfaces on the peptide are expected to be similar. This assertion is supported by similarities in the distributions of polar anesthetics between the head group regions and the hydrocarbon cores of the GMO and phospholipid bilayers.[46,48]

Conformational equilibria of the blocked peptides at the interface are different from those in the gas phase or in bulk water. At the interface, five different states correspond to free energy minima in $P(\phi,\psi)$: α_R, β, α_L, C_5, and C_{7-ax}. The first two are also stable in water, whereas the latter two are stable in the gas phase. As reported in Table 3, the relative free energies of the different states depend on the nature of the side chain. NANML is predominantly in the β conformation, but with significant contributions from C_5 and α_R. In contrast, the

most favored conformation of NANMQ is α_R, followed by C_5 and β. In NANMA, these three conformations are almost equally populated.

Just like in water, the solvent effect at the interface destabilizes β', compared to α_R. Interestingly enough, the relative interfacial free energies of solvation of the β' state are nearly identical for the three peptides and equal to 1.6−1.8 kcal/mol. For NANML and NANMA, these free energies are smaller than the free energies of solvation in water. This is an expected result. At the interface, water molecules solvate the peptides only partially, and therefore, a more polar α_R conformer gains less stabilization, compared to the β' state, from interactions with the surrounding medium than in bulk aqueous solution. For NANMQ, however, the opposite is true: α_R is more stable at the interface than in water. This indicates that the simple explanation of the solvent effect, based on changes in solute polarity, that worked well for aqueous solutions of the peptides, is insufficient for the interfacial environment. Clearly, other factors contribute significantly to the conformational equilibria at the interface. To understand these factors, we consider the conformational preferences of the side chain in NANMQ and its ability to form intramolecular hydrogen bonds. As we observed previously, in vacuum the side chain is almost always involved in hydrogen bonding with the backbone, whereas such bonds are virtually nonexistent in an aqueous solution. In general, intramolecular hydrogen bonds are destabilized in polar surroundings. This implies that the fraction of peptide configurations with intramolecular hydrogen bonds involving the side chain is lower at the interface than in a vacuum, but higher than in water. This is indeed the case; the fraction varies between 50 and 65%, depending on the conformation of the backbone. Since only atoms removed from water form intramolecular hydrogen bonds, the relative populations of the different bonds and the accompanying side chain conformations at the interface do not need to be the same as in the gas phase. This is observed for both α_R and β', but is particularly clear in the latter state. The $N_7-H\cdots O{=}C_\delta$ hydrogen bond, which is the most common in both conformations in the gas phase, is markedly depopulated at the interface. It still remains, however, the most frequently encountered intramolecular hydrogen bond in the α_R conformation, but disappears almost completely in β'. In contrast, the most populated hydrogen bond for β' at the interface is $O_{12}\cdots H-N-C_\delta$, which is virtually nonexistent in the gas phase. A similar, but not nearly as pronounced, shift in the hydrogen-bonding pattern is observed for α_R. The $O_{12}\cdots H-N-C_\delta$ bond is frequent at the interface, but is also occasionally found in the gas phase. In general, if NANMQ is moved from the gas phase to the interface, the pattern of hydrogen bonds involving the side chain changes, thereby inducing conformational changes around the χ angles. This is clearly shown in Figure 6. The changes lead to the increase of the internal free energy of the peptide. Since the changes are larger in β' than in α_R, they contribute to the observed destabilization of the former state at the interface.

The discussion above illustrates that the interface exerts specific, unique effects on conformational equilibria. Even though conformations stable in both bulk phases are also stable in the interfacial environment, $P(\phi,\psi)$ at the interface cannot be simply represented as weighted averages of the distributions in the bulk phases. The effect of the interface on the orientational distributions of the peptides is even more pronounced. One way to notice this effect is by examining the angle θ between the interface normal, pointing toward water, and the side chain vector, directed from C_α to C_β, C_γ, or C_δ for

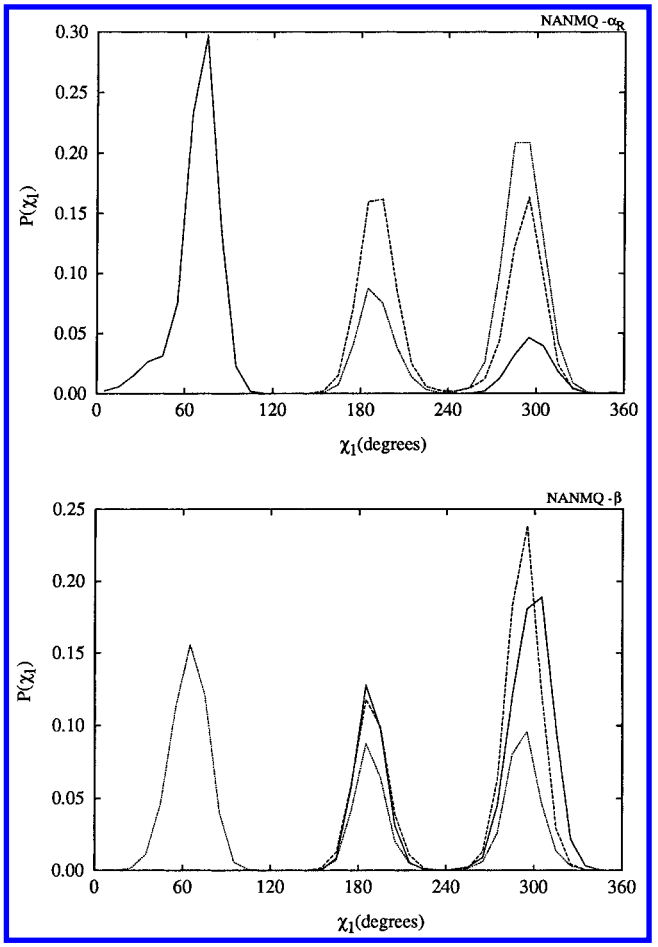

Figure 6. Probability distributions of finding NANMQ at different values of the side chain dihedral angle χ in the gas phase (solid line), in an aqueous solution (dashed line), and at the water−hexane interface (dotted line). Only the α_R (top) and the β (bottom line) states are displayed.

NANMA, NANML, and NANMQ, respectively. If the value of θ is less than 90°, the side chain is directed toward water, whereas θ greater than 90° corresponds to the side chain pointing toward hexane. The probability distribution, $P(\theta)$, is calculated as

$$P(\theta) = \frac{N_\theta}{N \sin\theta} \quad \text{and} \quad \sum_\theta P(\theta) \sin\theta = 1 \qquad (2)$$

where N_θ is the number of configurations with the side chain angle in the range $\theta \pm \delta\theta$ and N is the total number of configurations. Using this definition, $P(\theta)$ is normalized to describe the probability of finding the vector in the same solid angles at different values of θ. $P(\theta)$ for the three peptides in the α_R and β' conformations are shown in Figure 7. For NANML and NANMA the distributions are peaked near 180°, thus indicating that the nonpolar side chains are directed toward the nonpolar, hexane phase. As can be seen from Figure 8, a considerable free energy has to be expended to rotate the side chain toward water. This free energy, $\Delta A(\theta)$, defined as

$$\Delta A(\theta) = -k_B T \ln\frac{N_\theta}{N} \qquad (3)$$

is nearly constant between 100° and 180°, but increases rapidly for smaller angles, when the side chain becomes directed toward

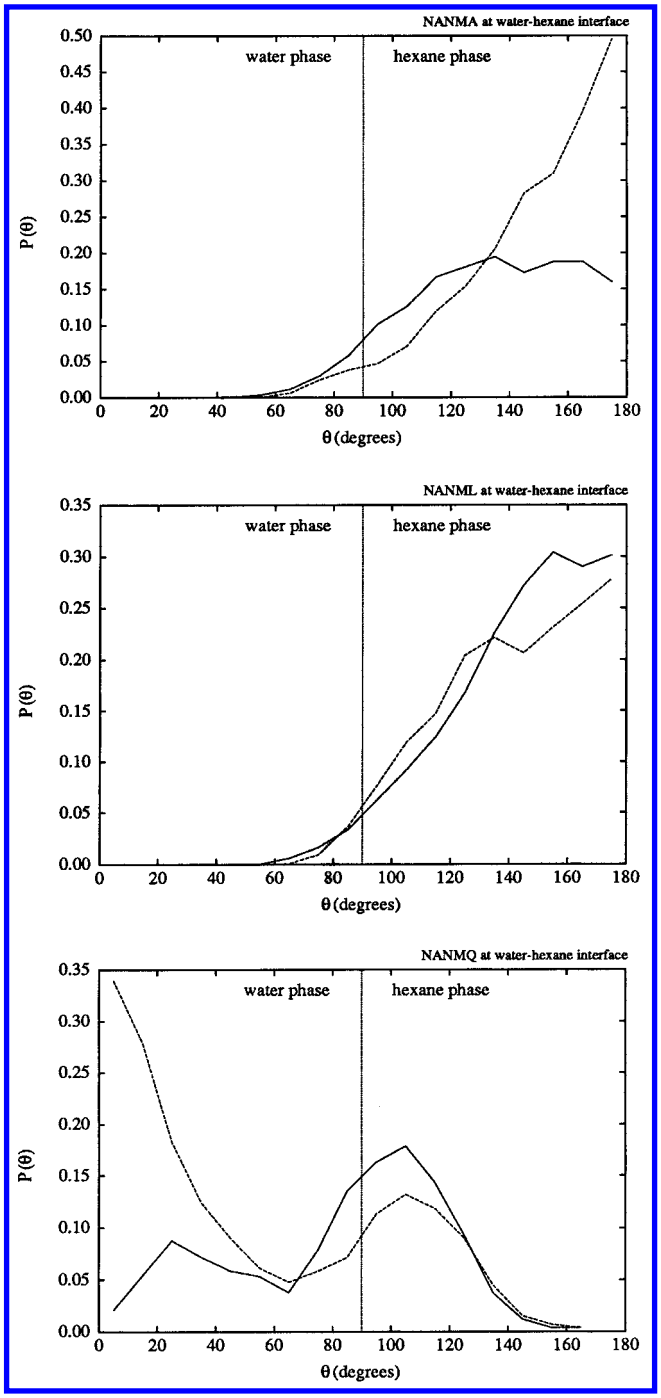

Figure 7. Probability distributions of the angle, θ, between the side chain of NANMA (top), NANML (middle), and NANMQ (bottom), with the normal to the interface. Only the α_R (solid line) and the β (dashed line) states are displayed.

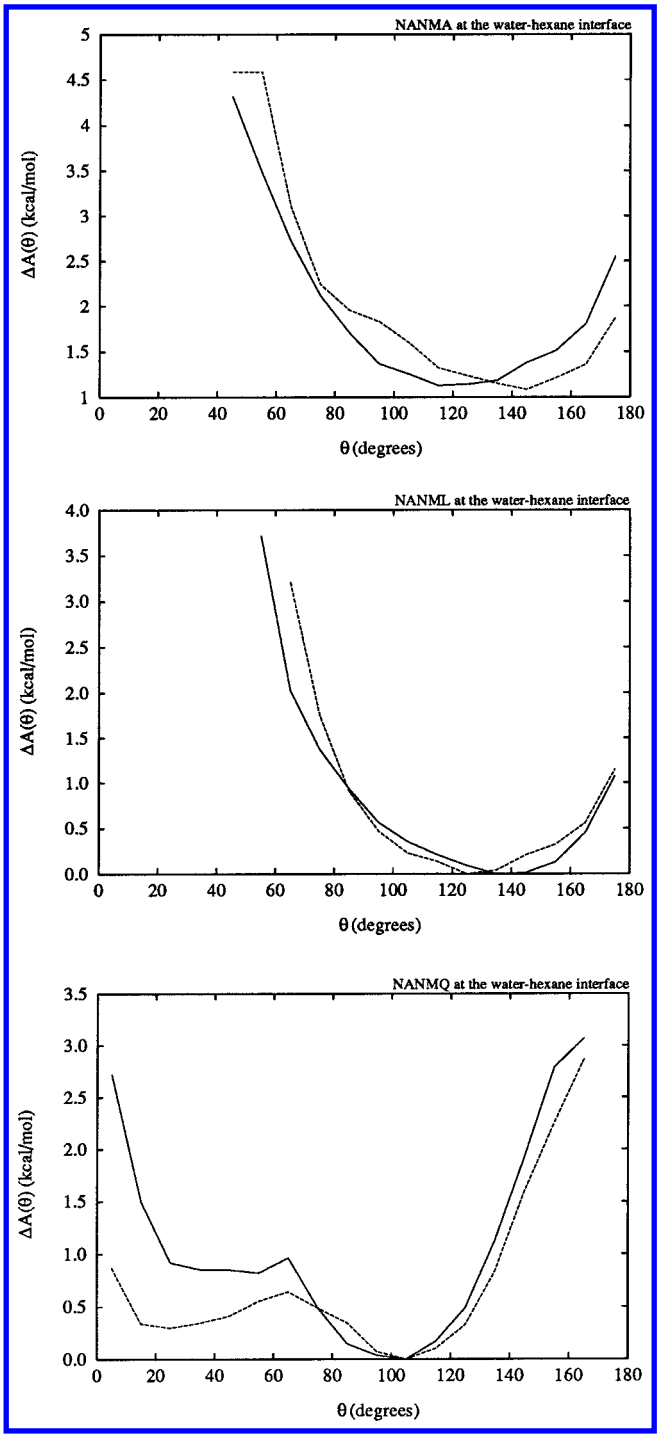

Figure 8. Free energy as a function of θ, the angle between the side chain of NANMA (top), NANML (middle), and NANMQ (bottom), and the normal to the interface. Only the α_R (solid line) and the β (dashed line) states are displayed.

water. For $\theta < 50°$, $\Delta A(\theta)$ is so large that no configurations in this range were observed during the simulations.

For NANMQ, $P(\theta)$ is quite different. The distribution exhibits two maxima, near 0 and 90°. They correspond, respectively, to the side chain directed toward water and parallel to the interface. One might inquire why the polar side chain is not always immersed in water. This is most likely due to the possibility of forming intramolecular hydrogen bonds between the side chain and the backbone. When the side chain is buried in water, such hydrogen bonds are disrupted. On the other hand, if the chain is approximately parallel to the interface, it is possible to retain both the hydrogen bonds and the partial hydration of the polar groups in the chain. As a result, these two orientations are energetically competitive. The orientation perpendicular to the interface dominates for β', whereas the parallel orientation is preferred for α_R. The perpendicular arrangement of the side chain is favored in the β' state mostly because it allows for a better shielding from water of the intramolecular hydrogen bond in C_5.

Compared to the bulk aqueous solution, the interfacial environment influences not only the conformational equilibria of blocked amino acids but also the dynamics of isomerization between the stable states. As noted previously,[11] the free energy barrier separating β from α_R in NANMA is lower at the interface. A similar effect is found for NANML. In both cases,

the reduction is equal to approximately 0.8−0.9 kcal/mol. In the transition-state approximation, this corresponds to a 2-fold increase in the rate constant of the isomerization reaction. In contrast, the barrier between the same two states in NANMQ increases at the interface by 0.5 kcal/mol.

Conclusion

Investigations of terminally blocked single amino acids with side chains of different polarity at the water−hexane interface provide valuable insights into the unique role of interfacial environments in mediating the structural organization of peptides, which are generally disordered in bulk solutions.[28,66] Although the model systems examined here are too small to involve side chain−side chain and long-range backbone interactions, which are essential in peptide folding, the results shed light on how interfaces influence intrinsic conformational preferences of peptide units with different sequences.

Concentrations of terminally blocked amino acids at interfaces between water and a nonpolar medium, such as hexane, are higher than in the adjacent nonpolar phases. This tendency to accumulate at the interface is independent of the polarity of the side chains; it is observed for nonpolar leucine, polar glutamine, and alanine, which represents an intermediate case. A similar interfacial activity was found for a broad range of small but nonamphiphilic solutes at different aqueous interfaces, using both experimental[43,51,52,67,68] and computational techniques.[46,48,50]

Conformational equilibria at interfaces are governed by a subtle interplay of several interactions, that *simultaneously* influence the stability of the peptides. This includes solute−solvent electrostatic interactions, which favor more polar conformations, usually characterized by larger dipole moments. These interactions are mainly responsible for the stabilization of α_R, relative to β, in water and, to a lesser degree, at the interface. The stabilization is markedly more pronounced for NANML and NANMA than for NANMQ, because the difference in the dipole moments between α_R and β is larger if a blocked amino acid has a nonpolar side chain. Other interactions that significantly affect conformational preferences are intramolecular hydrogen bonding involving side chains. These bonds are formed in NANMQ in a nonpolar environment, such as the gas phase or the hexane side of the interface. In the interfacial system, they favor α_R over β. The importance of intramolecular hydrogen bonding was also stressed in experimental studies of tripeptides at the water−membrane interface.[29] Since the interactions that determine conformational equilibria of blocked amino acids in either polar or nonpolar environments also influence their conformational preferences at the interface, conformations present in both isotropic environments are also stable in the interfacial region. The populations of different stable states at the interface, however, cannot be simply deduced from the populations in the bulk media. This is a consequence of the specific effects influencing conformational equilibria that are present only in the interfacial environment.

The most important feature of the interface is that the polar and nonpolar phases exist in proximity. As a result, hydrophilic and hydrophobic groups of the peptides can, at least partially, segregate into the polar and the nonpolar phases, respectively. This affects not only the conformation of the backbone but, most importantly, the orientation of the peptide at the interface. The nonpolar NANML and, to a lesser degree, NANMA adopt orientations that allow their nonpolar side chains to be buried in hexane, whereas NANMQ is oriented in such a way that its polar side chain is exposed toward water. The free energies needed to rotate each peptide to a position in which the side chain is parallel to the interface are modest, but increase rapidly with further rotation, as the side chain is moved to the solvent of different polarity. This indicates that interfacial folding of short peptides is strongly driven by their tendency to adopt amphiphilic structures. Whether these structures are ordered (e.g. α-helices or β-strands) depends on the sequence.

Extensions that build on the present work can be aimed in three directions: (1) including other, especially aromatic, side chains, (2) considering more complex interfacial systems, in particular those between water and phospholipid bilayer, and (3) investigating longer peptides, some of them capable of forming ordered secondary structures. Work along some of these lines is already in progress.[40]

Acknowledgment. This work was supported by a grant from the NASA Exobiology Program. C.C. was supported by a National Research Council Associateship at NASA−Ames Research Center. Computational resources from the National Aerodynamic Simulation facility (NAS) are gratefully acknowledged. We thank Drs. Michael A. Wilson and Michael H. New for helpful discussions.

References and Notes

(1) Rossky, P. J.; Karplus, M. *J. Am. Chem. Soc.* **1979**, *101*, 1913.
(2) Grant, J. A.; Williams, R. L.; Scheraga, H. A. *Biopolymers* **1990**, *30*, 929.
(3) Chipot, C.; Ángyán, J. G.; Maigret, B.; Scheraga, H. A. *J. Phys. Chem.* **1993**, *97*, 9797.
(4) Gould, I. R.; Cornell, W. D.; Hillier, I. H. *J. Am. Chem. Soc.* **1994**, *116*, 9250.
(5) Hagler, A. T.; Moult, J. *Nature* **1978**, *272*, 222.
(6) Brady, J.; Karplus, M. *J. Am. Chem. Soc.* **1985**, *107*, 6103.
(7) Mezei, M.; Mehrotra, P. K.; Beveridge, D. L. *J. Am. Chem. Soc.* **1985**, *107*, 2239.
(8) Ravishanker, G.; Mezei, M.; Beveridge, D. L. *J. Comput. Chem.* **1986**, *7*, 345.
(9) Anderson, A.; Hermans, J. *Proteins* **1988**, *3*, 262.
(10) Tobias, D. J.; Brooks, C. L. *J. Phys. Chem.* **1992**, *96*, 3864.
(11) Pohorille, A.; Wilson, M.A. Reaction dynamics in clusters and condensed phases. In *The Jerusalem symposia on quantum chemistry and biochemistry*; Jortner, J., Levine, R., Pullman, B., Eds.; Kluwer: Dordrecht, 1993; Vol. 26, p 207.
(12) Pellegrini, M.; Grønbech-Jensen, N.; Doniach, S. *J. Chem. Phys.* **1996**, *104*, 8639.
(13) Neria, E.; Fischer, S.; Karplus, M. *J. Chem. Phys.* **1996**, *105*, 1902.
(14) Pettitt, B. M.; Karplus, M. *Chem. Phys. Lett.* **1985**, *121*, 194.
(15) Pettitt, B. M.; Karplus, M. *J. Phys. Chem.* **1988**, *92*, 3994.
(16) Kaiser, E. T.; Kedzy, F. J. *Annu. Rev. of Biophys. Biophys. Chem.* **1987**, *16*, 561.
(17) Peng, Y.; Fisher, P. J.; Kemple, M. D. *Biophys. J.* **1996**, *70*, 2223.
(18) Schwyzer, R. *Biopolymers* **1991**, *31*, 785.
(19) Richardson, C. D.; Choppin, P. W. *Virology* **1983**, *131*, 518.
(20) Damodaran, K. V.; Merz, K. M., Jr.; Gaber, B. P. *Biophys. J.* **1995**, *69*, 1299.
(21) Baatz, J. E.; Smyth, K. L.; Whitsett, J. A.; Baxter, C.; Absolom, D. R. *Chem. Phys. Lipids* **1992**, *63*, 91.
(22) Johansson, J.; Szyperski, T.; Curstedt, T.; Wüthrich, K. *Biochemistry* **1994**, *33*, 6015.
(23) Terzi, E.; Hölzemann, G.; Seelig, J. *J. Mol. Biol.* **1995**, *252*, 633.
(24) Randall, L. L.; Hardy, S. J. S. *Science* **1989**, *243*, 1156.
(25) Jones, J. D.; McKnight, J. C.; Gierasch, L. M. *J. Bioenerg. Biomembr.* **1990**, *22*, 213.
(26) Tamm, L. K. *Biochim. Biophys. Acta* **1991**, *1071*, 123.
(27) DeGrado, W. F.; Lear, J. D. *J. Am. Chem. Soc.* **1985**, *107*, 7684.
(28) Erne, D.; Sargent, D. F.; Schwyzer, R. *Biochemistry* **1985**, *24*, 4261.
(29) Jacobs, R. E.; White, S. H. *Biochemistry* **1989**, *28*, 3421.
(30) Parente, R. A.; Nadasdi, L.; Subbarao, N. K.; Szoka, F. C. *Biochemistry* **1990**, *29*, 8713.
(31) Brown, J. W.; Huestis, W. H. *J. Phys. Chem.* **1993**, *97*, 2967.
(32) Wimley, W. C.; White, S. H. *Nature Struct. Biol.* **1996**, *3*, 842.
(33) Damodaran, K.V.; Merz, K. M., Jr. *J. Am. Chem. Soc.* **1995**, *117*, 6561.
(34) Kato, T.; Lee, S.; Ono, S.; Agawa, Y.; Aoyagi, H.; Ohno, M.; Nishino, N. *Biochim. Biophys. Acta* **1991**, *1063*, 191.

(35) Lu, S.; Ciardelli, T.; Reyes, V. E.; Humphreys, R. E. *J. Biol. Chem.* **1991**, *266*, 10054.
(36) Chung, L. A.; Lead J. D.; Degrado, W. F. *Biochemistry* **1992**, *31*, 6608.
(37) Ono, S.; Lee, S.; Mihara, H.; Aoyagi, H.; Kato, T.; Yamasaki, N. *Biochim. Biophys. Acta* **1990**, *1022*, 237.
(38) Macquaire, F.; Baleux, F.; Giaccobi, E.; Huynh-Dinh, T.; Neumann, J. M.; Sanson, A. *Biochemistry* **1992**, *31*, 2576.
(39) Pohorille, A.; Wilson, M. A. Interaction of a model peptide with a water-bilayer system. In *Structure and reactivity in aqueous solution: characterization of chemical and biological systems*, Cramer, C., Truhlar, D., Eds.; ACS Symposium Series No. 568; ACS: Washington, DC, 1994; Chapter 11, p 395.
(40) Chipot, C.; Pohorille, A. *J. Mol. Struct. (THEOCHEM)* **1997**, *398*, 529.
(41) Gallusser, A.; Kuhn, A. *EMBO J.* **1990**, *9*, 2723.
(42) Mosior, M.; McLaughlin, S. *Biochim. Biophys. Acta* **1992**, *1105*, 185.
(43) Wimley, W. C.; White, S. H. *Biochemistry* **1993**, *32*, 6307.
(44) Beschiaschvili, G.; Seelig, J. *Biochemistry* **1992**, *31*, 12813.
(45) Dathe, M.; Schumann, M.; Wieprecht, T.; Winkler, A.; Beyermann, M.; Krause, E.; Matsuzaki, K.; Murase, O.; Bienert, M. *Biochemistry* **1996**, *35*, 12612.
(46) Pohorille, A.; Wilson, M. A., *J. Chem. Phys.* **1996**, *104*, 3760.
(47) Blondelle, S. E.; Ostreh, J. M.; Houghten, R. A.; Perez-Paya, E. *Biophys. J.* **1995**, *68*, 351.
(48) Pohorille, A.; Cieplak, P.; Wilson, M. A. *Chem. Phys.* **1996**, *204*, 337.
(49) Chipot, C.; Wilson, M. A.; Pohorille, A. *J. Phys. Chem. B* **1997**, *101*, 782.
(50) Pohorille, A.; Wilson, M. A.; Chipot, C. Interaction of alcohols and anesthetics with the water−hexane interface: A molecular dynamics study. In *Progress in colloid and polymer science*; Texter, J., Ed.; 1997; Vol. 103, p 29.
(51) North, C.; Cafiso, D. S. *Biophys. J.* **1997**, *72*, 1754.
(52) Tang, P.; Yan, B.; Xu, Y. *Biophys. J.* **1997**, *72*, 1676.
(53) Jorgensen, W. L.; Chandrasekhar, J.; Madura, J. D.; Impey, R. W.; Klein, M. L. *J. Chem. Phys.* **1983**, *79*, 926.
(54) Jorgensen, W. L.; Madura, J. D.; Swenson, C. J. *J. Am. Chem. Soc.* **1984**, *106*, 6683.
(55) Ryckaert, J.; Cicotti, G.; Berendsen, H. J. C. *J. Comput. Phys.* **1977**, *23*, 327.
(56) Cornell, W. D.; Cieplak, P.; Bayly, C. I.; Gould, I. R.; Merz, K. M., Jr.; Ferguson, D. M.; Spellmeyer, D. C.; Fox, T.; Caldwell, J. C.; Kollman, P. A. *J. Am. Chem. Soc.* **1995**, *117*, 5179.
(57) Wilson, M.; Pohorille, A. *J. Am. Chem. Soc.* **1994**, *116*, 1490.
(58) Owenson, B.; Pohorille, A. COSMOS—*A software package for COmputer Simulations of MOlecular Systems*. NASA—Ames Research Center, Moffett Field, CA 94035-1000, 1987.
(59) Verlet, L. *Phys. Rev.* **1967**, *159*, 98.
(60) Allen, M. P.; Tildesley, D. J. *Computer Simulation of Liquids*; Clarendon Press: Oxford, 1987.
(61) Torrie, G. M.; Valleau, J. P. *J. Chem. Phys.* **1977**, *66*, 1402.
(62) Valleau, J. P.; Card, D. N. *J. Chem. Phys.* **1972**, *57*, 5457.
(63) Kumar, S.; Rosenberg, J. M.; Bouzida, D.; Swendsen, R. H.; Kollman, P. A. *J. Comput. Chem.* **1995**, *16*, 1339.
(64) Madison, V.; Kopple, K. D. *J. Am. Chem. Soc.* **1980**, *102*, 4855.
(65) Smaby, J. M. *Biophys. J.* **1990**, *58*, 195.
(66) Schwyzer, R. *Biochemistry* **1986**, *25*, 4281.
(67) Baber, J.; Ellena, J. F.; Cafiso, D. S. *Biochemistry* **1995**, *34*, 6533.
(68) Xu, Y.; Teng, P. *Biophys. Biochim. Acta* **1997**, *1323*, 154.